Sustainable Process Design and Synthesis of Hydrocarbon Biorefinery through Fast Pyrolysis and Hydroprocessing

Qiao Zhang, Jian Gong, Matthew Skwarczek, Dajun Yue, and Fengqi You
Dept. of Chemical and Biological Engineering, Northwestern University, Evanston, IL 60208

DOI 10.1002/aic.14344
Published online January 16, 2014 in Wiley Online Library (wileyonlinelibrary.com)

The process design and synthesis of hydrocarbon biorefinery, which is composed of fast pyrolysis, biocrude collection, hydroprocessing and hydrogen production sections, under economic and environmental considerations are concerned. A superstructure is developed that includes multiple process alternatives in each stage of the process flow diagram. A bi-criteria mixed integer nonlinear programming model is proposed to maximize the economic performance measured by the net present value and minimize the global warming potential according to life cycle assessment procedures. The bi-criteria mixed integer nonlinear programming model is solved with the ε-constraint method, and the resulting Pareto curve reveals the trade-off between the economic and environmental performance of the process. The two selected "good choice" optimal designs indicate net present values of 573 and 93.6 $MM (unit costs of $3.43 and $5.26 per gallon of gasoline equivalent), corresponding to global warming potentials of 100 and 53 kton CO_2 equivalent per year (unit greenhouse emissions of 1.95 and 2.04 kg CO_2 per gallon of gasoline equivalent), respectively. © 2014 American Institute of Chemical Engineers *AIChE J*, 60: 980–994, 2014

Keywords: superstructure, fast pyrolysis, hydroprocessing, hydrogen production, mixed integer nonlinear programming, life cycle assessment

Introduction

Although modern civilization owes much to petroleum and its chemical derivatives, it is environmental unfriendly and quickly becoming a diminishing energy resource. Among all currently available renewable energy alternatives, biofuel emerges as the most promising near-term solution to the country's increasing environmental concerns and heavy dependence on imported oil.[1] Therefore, the U.S. government passed the Energy Independence and Security Act (EISA) of 2007 to spur the development of biofuel industry, which requires the annual biofuel production capacity to increase from 4.7 billion gallons in 2007 to 36 billion gallons by 2022.[2] With the most recent biofuel technologies, biomass-derived hydrocarbon fuels can now be produced from a wide variety of cellulosic materials such as agricultural residues, wood residues, and energy crops.[3] The most critical advantage of hydrocarbon biofuels is that they are chemically similar and functionally identical to conventional fossil fuels (e.g., gasoline, diesel, jet fuel), thus perfectly compatible with the existing distribution infrastructure and vehicle engines.[4]

Various pathways for the production of hydrocarbon biofuels were proposed and improved by researchers in the past decades, among which the pyrolysis pathway is recognized as a promising option that can help the nation to achieve the EISA requirement in a sustainable and cost-effective way.[5] However, to reach commercial-scale production of hydrocarbon biofuels, several challenges in the design and operation of hydrocarbon biorefineries need to be overcome.[6] From the perspective of economic performance, it requires the effective synthesis of a complicated process network and efficient integration of utility resources. Specifically, due to the high cost and considerable consumption of hydrogen in pyrolysis biorefineries, technical options for the design of hydroprocessing and hydrogen production sections need to be addressed. Conversely, the environmental impact of a process design is of equal importance. Since hydrocarbon biofuels are projected as sustainable energy solutions, it is important to carefully assess the environmental sustainability and avoid adverse implications of the biorefinery.[7] However, only a limited number of existing works have considered environmental sustainability issues in their process design for biorefineries. This is partially because of the lack of effective modeling framework that can integrate the environmental evaluation tools with the state-of-the-art process design and optimization tools, which is consequently the focus of this work.

In this article, we develop a superstructure for the design and synthesis of hydrocarbon biorefinery through fast pyrolysis and hydroprocessing. The biorefinery design consists of four major parts, including fast pyrolysis,[8] biocrude collection,[9] hydroprocessing,[8] and hydrogen production.[9] Different options are considered in hydroprocessing and hydrogen production sections, leading to a number of production pathways. For hydroprocessing, three types of technologies are

Additional Supporting Information may be found in the online version of this article.

Correspondence concerning this article should be addressed to F. You at you@northwestern.edu.

considered with different catalysts to produce gasoline and diesel products. In addition, we consider that hydrogen can be produced from three options: natural gas steam reforming, biocrude steam reforming, or biomass gasification. A mixed integer nonlinear programming (MINLP) model for the optimization of the superstructure-based biorefinery is established and solved. The optimization objective of the MINLP model is to simultaneously maximize the net present value (NPV) and minimize the global warming potential (GWP) by considering mass balance, energy balance, economic analysis, and environmental evaluation constraints. The ε-constraint method is introduced to make trade-offs between NPV and GWP, and then generate Pareto-optimal solutions that constitute the Pareto curve. Decision variables on the process design options and technologies, equipment placement, production capacity, feedstock and utilities consumption, as well as the flow rates of all streams involved are determined under both the economic and environmental considerations. The environmental impact indicator GWP is used to measure the gate-to-gate greenhouse gas (GHG) emissions of the biorefinery within the project lifetime. Life cycle inventories (LCI) of direct and indirect emissions are assessed to serve as the basis for environmental evaluation.

The novelties of this work are summarized below:

- A novel process superstructure for the sustainable design and operation of hydrocarbon biorefinery based on fast pyrolysis, hydroprocessing, as well as hydrogen production.
- An MINLP model that simultaneously optimizes the economic and environmental performance of the entire hydrocarbon biorefinery using the life cycle optimization (LCO) framework.
- Insights and suggestions for future developments based on the resulting Pareto-optimal curve, optimal process configuration, cost, emission profile, and so forth.

The remaining article is organized as follows. We first review the relevant literature. Then we propose a detailed process superstructure of the biorefinery, followed by a brief introduction about economic performance and environmental evaluation. Next, the problem statement is presented. The economic and environmental objective functions, as well as the solution method are given afterward. The optimization results are discussed to develop insights and suggestions. Conclusions are placed at the end.

Literature Review

Several techno-economic reports are available at National Renewable Energy Laboratory on both gasification and pyrolysis pathways.[10–13] Whereas, in this section, we will focus on the review of relevant works that use mathematical programming method for the optimization of design and operation of biomass-based energy systems. Sammons et al.[14] proposed a mathematical optimization-based framework to evaluate the profitability of biorefinery. Liu et al.[15] set up a multiobjective MINLP optimization model for the design of a polygeneration energy system producing both methanol and electricity from different coal feedstock. Chen et al.[16,17] addressed the optimal design and operation of polygeneration systems using coal and biomass to produce power, liquid fuels, and chemicals. The problem is formulated into a multiperiod MINLP optimization problem. Baliban et al.[18] proposed an MINLP model for the superstructure optimization of thermochemical conversion of combination of coal, natural gas, and biomass to liquid transportation fuels with heat and power integration considered. Martin and Grossmann[19] proposed an MINLP model for the conceptual design of the bioethanol production from switchgrass via gasification with a variety of options and synthetic pathways addressed. The same authors[20] proposed an MINLP model for the process design of Fisher–Tropsch diesel production from lignocellulosic switchgrass to minimize the energy and hydrogen consumptions.

Most of the works mentioned above consider economic performance as the only objective function, whereas a limited number of works have addressed the environmental sustainability issues. Liu et al.[15] proposed mixed integer linear programming models for optimal design of a polygeneration system that produces concurrently methanol and power using coal, natural gas, and biomass as raw materials. The NPV and environmental impact are simultaneously optimized using a multiobjective optimization framework. Wang et al.[21] proposed a multiobjective MINLP model for the superstructure optimization of a hydrocarbon biorefinery via gasification and Fisher–Tropsch synthesis under economic and environmental criteria. The superstructure considers alternative gasification technologies, syngas cooling, hydrogen production technologies, and Fisher–Tropsch synthesis catalysts. Gebreslassie et al.[22] proposed a bi-criteria nonlinear programming (NLP) model for the optimal design and operation of a hydrocarbon biorefinery via fast pyrolysis, hydrotreating, and hydrocracking of hybrid poplar wood feedstock considering economic and environmental performances. The model is solved by simultaneously maximizing the NPV and minimizing the environmental impacts. The environmental criterion is measured with GWP metric according to the life cycle assessment (LCA) procedures. Recently, Gebreslassie et al.[23] proposed a multiobjective MINLP model for the algae-based biorefinery considering aspects of biofuel production, power generation, and carbon sequestration under economic and environmental concerns. Daoutidis et al.[24] addressed the systems challenges of designing, deploying, and operating biorefineries at various levels. EI-Halwagi et al.[25] introduced a new approach for the incorporation of safety criteria into selection, location, and sizing of a biorefinery. Pham and EI-Halwagi[26] proposed a novel and systematic two-stage approach to the synthesis and optimization of a biorefinery. Ng et al.[27] introduced multiobjective fuzzy optimization for the synthesis of biorefinery considering economic, environmental, inherent safety, and inherent occupational health performances simultaneously to enhance the flexibility and reduce the overall cost.

Superstructure Configuration

In this article, a superstructure is proposed for the optimal design of hydrocarbon biorefinery through fast pyrolysis and hydroprocessing. The process flow diagram is shown in Figure 1. Four major sections, including fast pyrolysis, biocrude collection, hydroprocessing, and hydrogen production shown by red dashed rectangles in Figure 1, are used to perform the production of hydrocarbon biofuels. The fast pyrolysis section includes equipment units of dryer, pyrolyzer, and combustor. The biocrude collection section includes equipment units of cyclone, quench, and demister. The hydroprocessing section includes a two-stage hydrotreater to stabilize the biocrude via hydrodeoxygenation and decarboxylation, and a series of reaction and separation units including high and

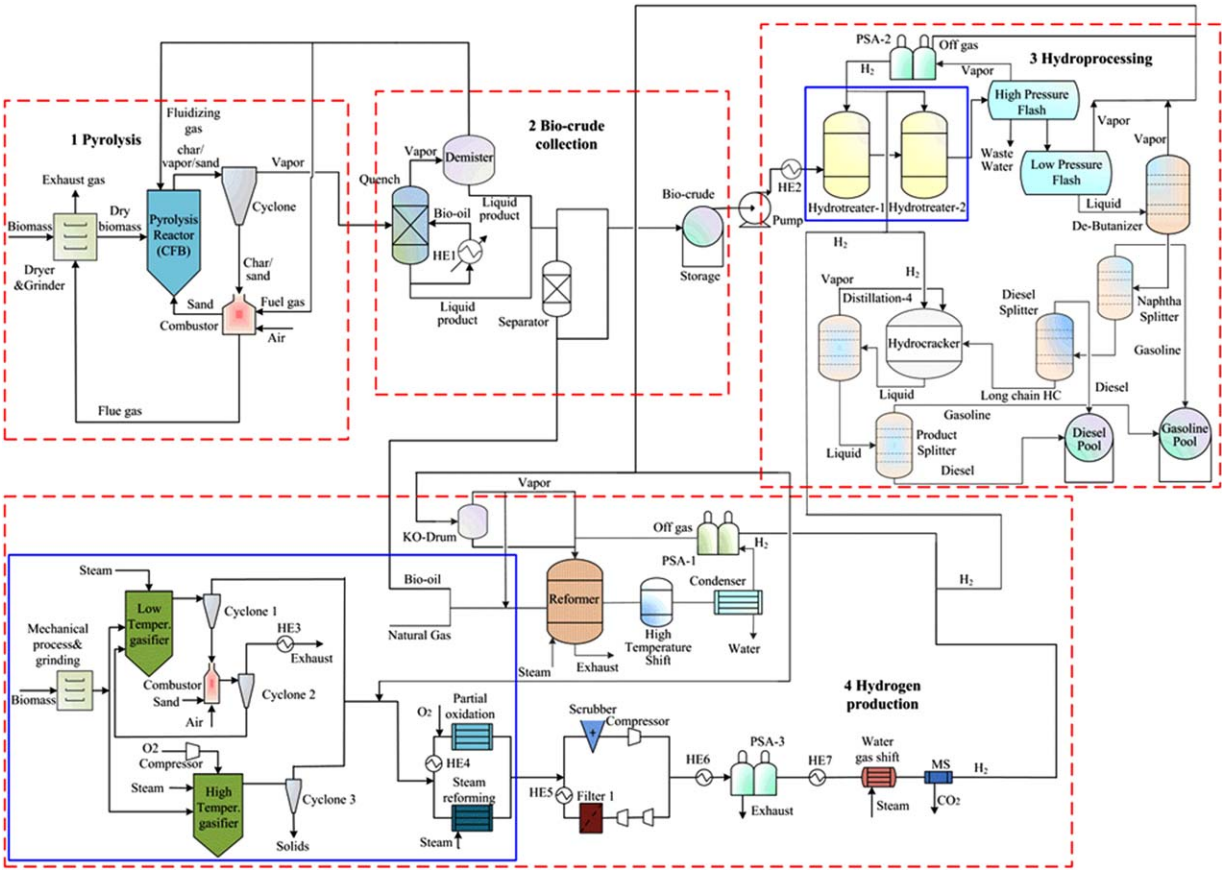

Figure 1. Complete superstructure-based process flow diagram of hydrocarbon biorefinery.

[Color figure can be viewed in the online issue, which is available at wileyonlinelibrary.com.]

low pressure flashes, pressure swing adsorption 2 (PSA2), debutanizer, naphtha splitter, diesel splitter, hydrocracker, product distillation column, and product splitter. For hydroprocessing feed highlighted by blue solid rectangle on the top right in Figure 1, we consider three options, corresponding to three hydroprocessing technologies with respective catalysts and feedstock options, derived from different design reports.[12,28–30] Besides, we consider three technologies in the hydrogen production section highlighted by blue solid rectangle on the bottom left in Figure 1. The first technology is natural gas steam reforming, including equipment units of steam reformer, high temperature shift, condenser, and PSA1. The second technology is biocrude steam reforming, with the equipment same as that in natural gas steam reforming. The third technology is biomass gasification, including equipment units of gasifier, cyclone, tar reformer, gas cleanup, PSA3, water gas shift, and membrane separation. Detailed discussion of each unit involved in the hydrocarbon biofuel production process will be presented below.

Fast pyrolysis

At the pyrolysis section, the raw biomass materials, moisture hybrid poplar wood in this work, is first sent to the contact dryer to decrease the water content from received 50 wt % to desired 7 wt %. The dried biomass is then ground to 2–6-mm size particles, to increase the heat-transfer area and speed up the pyrolysis reaction. The dried and ground biomass is heated in a circulating fluidized-bed pyrolyzer and then rapidly cooled to stop the side reaction. In the fast pyrolysis reactor, the biomass particles are decomposed to char solid, gas, and a liquid phase mainly including oxygenated hydrocarbons. The respective proportion of the three phases changes depending on the temperature and residence time of the reactants. Generally, higher temperature leads to more gas phase and longer residence time results in more char solid. Therefore, to increase the liquid yield,[8] moderate temperature (520°C) and short residence time (2 s) is favored, which is thereby named fast pyrolysis technology. Meanwhile, sand is used as heat carrier. Part of the gas is recycled as fluidizing gas into the pyrolyzer and the rest is used as fuel gas in the combustor to reheat the sand. The process flow diagram of fast pyrolysis section is shown in Figure 2.

Biocrude collection

After the fast pyrolysis, the triphasic product is high in temperature and the existence of char solid can lead to the decomposition of oxygenated hydrocarbons. Therefore, the triphasic product must be cooled and separated immediately to avoid side reactions. Cyclone is first introduced to remove the solids consisting of sand and char. Sand and char are recycled for combustion. The oxygenated hydrocarbons collected from the cyclone are rapidly quenched with the cooled biocrude and then separated from the gas phase. The separated gas from quench is further sent to demister to further collect the oxygenated hydrocarbons in the gas phase. After demister, most gas is sent back to the pyrolyzer as fluidizing gas and the remaining as fuel gas to the combustor.

The liquid from the quench and that from the demister are mixed together to form the intermediate product: biocrude.

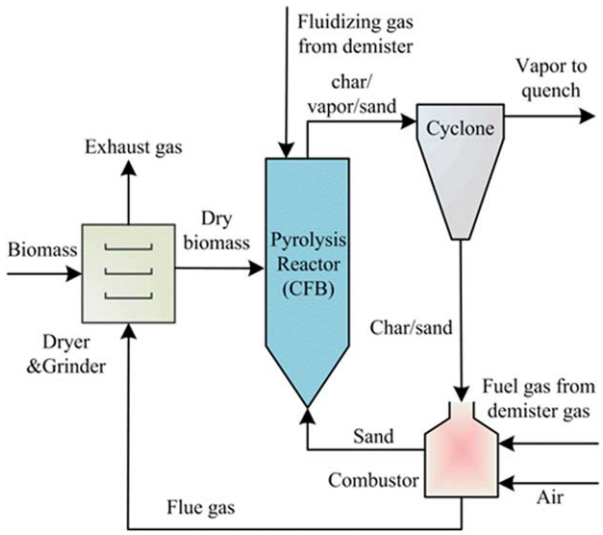

Figure 2. Process flow diagram of fast pyrolysis section.

[Color figure can be viewed in the online issue, which is available at wileyonlinelibrary.com.]

The biocrude is composed of oxygenated hydrocarbons within the range of C_2–C_{12}, as well as about 20–25 wt % water content. The process flow diagram of biocrude collection section is shown in Figure 3.

Hydroprocessing

Compared to conventional gasoline and diesel products, the oxygenated hydrocarbons are relatively high in oxygen content and products with such molecular structure cannot be used directly as fuel substitute. According to the difference in oxygen content, biocrude can be divided into two kinds of compound. One is water soluble oil, making up about 50–70 wt % of the biocrude and the other is pyrolytic lignin, making up 30–50 wt %. The oxygen content in water soluble oil (up to 60 wt %) is much higher than that in pyrolytic lignin (up to 30 wt %).[28] As aforementioned, oxygen content must be removed to stabilize the biocrude by hydroprocessing, consisting of hydrotreating and hydrocracking.

In this work, we consider three hydroprocessing feedstock options. The three hydroprocesing feedstock options are derived from three process design reports, respectively.[12,29,30] In option (a), the biocrude is fully utilized for hydroprocessing and cobalt molybdenum (CoMo) is chosen as the catalyst.[12] First, the biocrude is pumped and mixed together with high-pressure hydrogen, and then heated to the temperature of reaction. In hydrotreating, a two-stage hydrotreater is used. The first stage serves to stabilize the biocrude by mild hydrotreating over CoMo.[12] The second stage uses the same catalyst, but the oil product from the first stage is further hydrotreated at a higher temperature. After hydrotreating, the stabilized biocrude is separated into short and long chains hydrocarbon products by consecutive splitters and distillation columns. The gasoline range products are mixed together. The long chain hydrocarbons are sent to the hydrocracker for further breaking down to produce both gasoline and diesel range products, which are separated afterward by distillation column and product splitter. At last, the gasoline and diesel products are sent to their respective storage. In option (b), only part of water soluble pyrolysis oil is used for hydrogen production and the rest is utilized for hydroprocessing, in which palladium on carbon (PdC) is chosen as the catalyst.[29] Note that we assume the hydrogen produced is dependent on the hydrogen demand in hydroprocessing. The rest of the process is identical to that in the first option. Option (c) is similar to the second option, except that nickel molybdenum (NiMo) is chosen as the catalyst for hydroprocessing.[30] When the second or third option is used, part of the water soluble oil is separated and fed to the steam reformer, and the remaining water soluble oil is fed to first-stage hydrotreating. Meanwhile, the pyrolytic lignin is used as the feed for second-stage hydrotreating. The difference between these two options is only in the split fraction of water soluble oil and the selection of second-stage hydrotreating catalyst, because of the use of different processing pathways.[28–31] Note that the first-stage hydrotreating always uses the CoMo catalyst. After hydrotreating, the products from the two hydrotreaters are mixed together and then sent to separation columns and splitters to produce the gasoline and diesel products.

After hydrotreating, the products are sent to high pressure flash. At the high pressure flash, the upgraded bio-oil is separated into bio-oil, waste water, and off-gas streams. The off-gas stream from high pressure flash is separated in PSA2 to recover hydrogen, which is reused in both hydrotreaters (see Figure 1). The bio-oil stream is sent to the low pressure flash. In low pressure flash, the incoming stream from the high pressure flash gets further separated into a liquid bio-oil stream and an off-gas vapor stream. After leaving the low pressure flash, the liquid bio-oil is separated by the debutanizer to remove light hydrocarbons, for example, butane, as they cannot be used as part of gasoline or diesel.

The output bio-oil from the debutanizer is then split into heavy and light fractions in the naphtha splitter, with the light fraction being the gasoline and the heavy fraction to be further separated in the diesel splitter. In the diesel splitter, the heavy fraction from the naphtha splitter is split into diesel stream as well as a heavy, long chain hydrocarbon stream: the

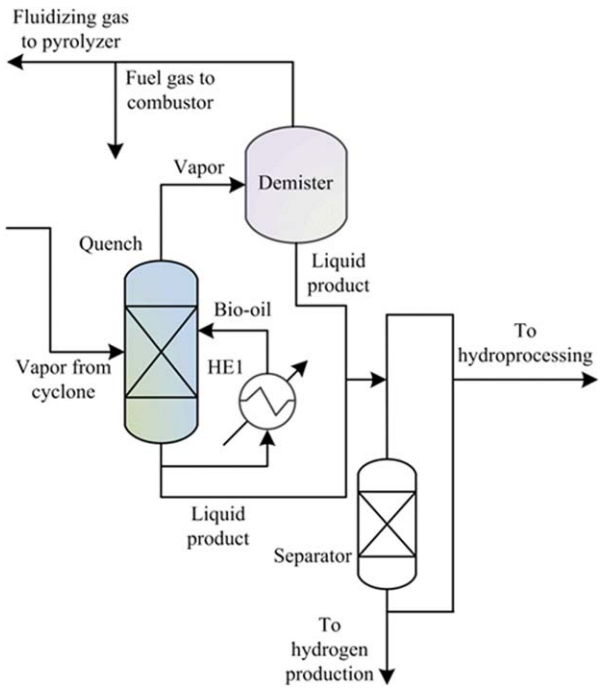

Figure 3. Process flow diagram of biocrude collection section.

[Color figure can be viewed in the online issue, which is available at wileyonlinelibrary.com.]

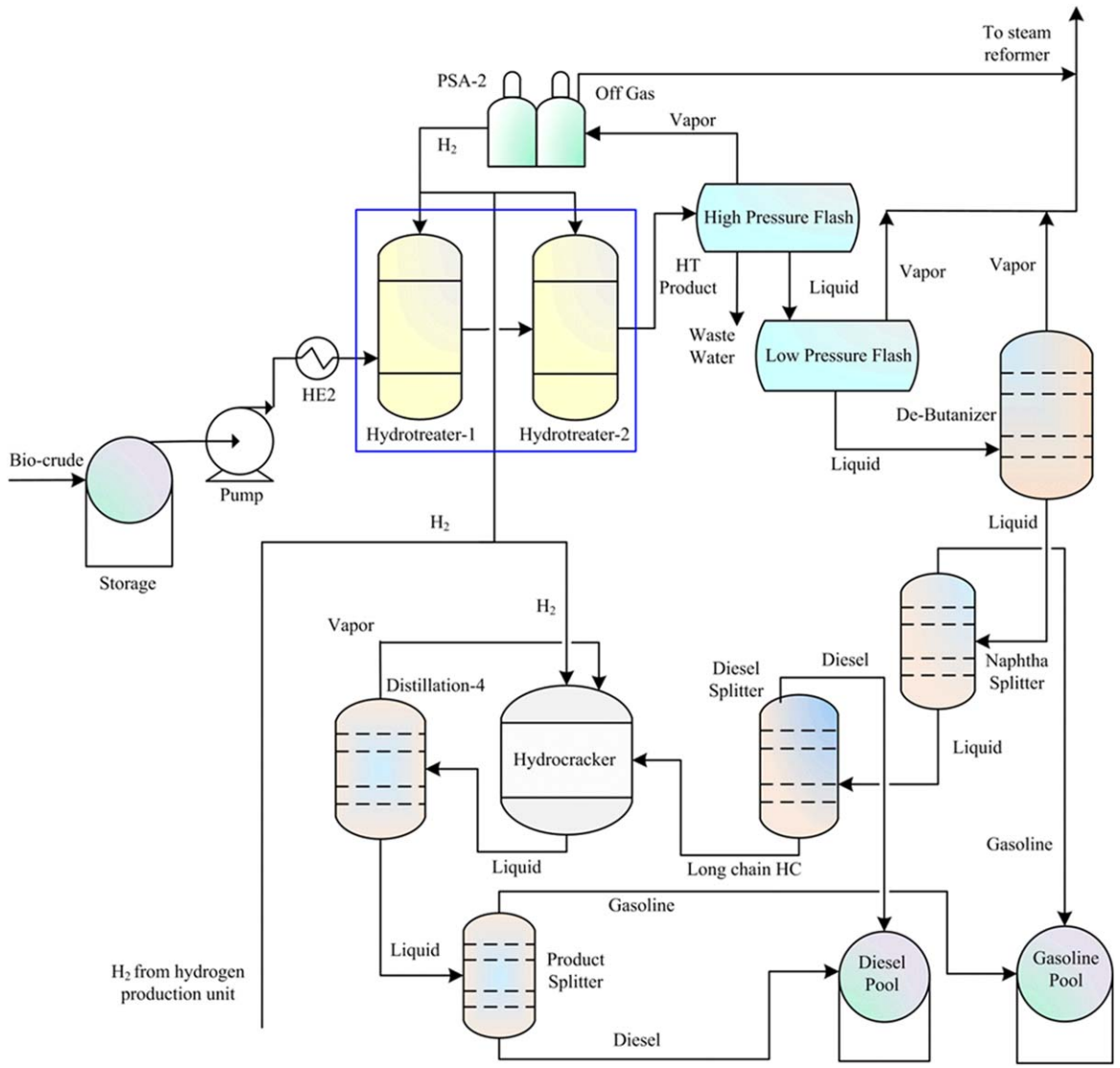

Figure 4. Process flow diagram of hydroprocessing section.

[Color figure can be viewed in the online issue, which is available at wileyonlinelibrary.com.]

latter must be further refined to be used as a fuel in hydrocracker. In the hydrocracker, the long chain hydrocarbons are broken down by hydrogen and the vapor products from the distillation column-4 are broken up into gasoline and diesel biofuels. After leaving the hydrocracker, the liquid product stream is split into vapor and liquid streams in distillation column-4 so that the vapor products can be recycled back to the hydrocracker to save the hydrogen consumption, and the liquid product stream goes on to be split into gasoline and diesel streams in the product splitter. In the product splitter, the liquid stream from the distillation column-4 is split into the lighter gasoline stream and heavier diesel stream. Finally, all gasoline range streams are mixed together and then sent to gasoline pool to form the gasoline product. The same case also applies for diesel streams to get the diesel product in diesel pool. The process flow diagram of hydroprocessing section is shown in Figure 4.

Hydrogen production

Hydrogen can be produced from natural gas, biocrude, or biomass. Natural gas steam reforming is traditionally used for hydrogen production due to its low production cost. However, natural gas is not a renewable resource thus not considered environmentally sustainable. In contrast, biomass can also be used to produce hydrogen in a sustainable way, though with a relatively higher cost than using natural gas. Besides, water soluble oil in the biocrude is biomass derived and can also be converted to hydrogen by steam reforming.[32]

When hydroprocessing feedstock option (a) is selected, the hydrogen can be produced from natural gas or biomass. Otherwise, in the cases of option (b) or (c), the hydrogen is produced only from the other part of biocrude via steam reforming, because the heterogeneous feedstock like the mixture of biocrude and nature gas is not tested in the literature. For natural gas steam reforming, as shown in Figure 5, the feed is a mixture of natural gas and some off-gas streams from the hydrotreating and hydrocracking processes. First, the mixture feed is sent to the steam reformer, in which the light hydrocarbons are mainly converted to carbon monoxide and hydrogen by steam. The heat is supplied by burning the process off-gases, which are the vents and off-gases of other separators, in the furnace. After steam reforming, the product is sent to the high temperature shift, in which the water gas

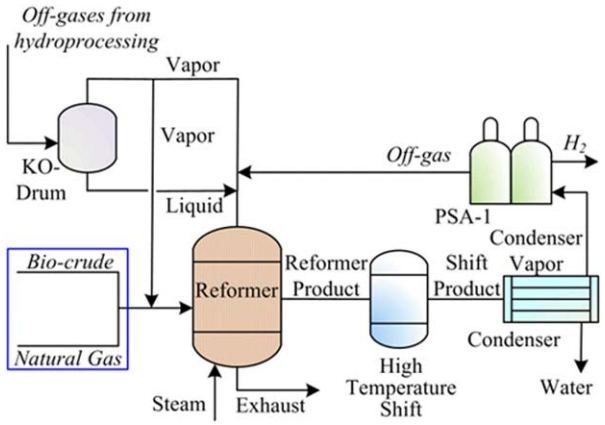

Figure 5. Process flow diagram of steam reforming.

[Color figure can be viewed in the online issue, which is available at wileyonlinelibrary.com.]

shift reaction converts the carbon monoxide and steam to carbon dioxide and hydrogen to increase the conversion of carbon monoxide to carbon dioxide. The product from high temperature shift is then separated by PSA to get high purity hydrogen for hydroprocessing and off-gas sent to the furnace of steam reforming for burning.

For the case of hydrogen production from biomass,[33,34] the process flow diagram shown in Figure 6 is considerably different from the one mentioned above. In such case, the biomass feedstock, dried switchgrass, is first fed to the gasifier, which can be of high temperature or low temperature. For low-temperature gasifier,[33] steam is also needed to supply the heat for gasification and then similar to pyrolysis, a cyclone is used to separate the gas components from the char, which is recycled and burned in the combustor for heating the steam. For high-temperature gasifier,[34] beside steam, oxygen is also required in gasification, so as to supply heat for vaporizing the biomass. After high-temperature gasification, the product is separated directly by the cyclone and combustor is not needed. After gasification and cyclone separation, the gas product consists of hydrogen, water, carbon monoxide, carbon dioxide, and some light hydrocarbons. Next, the gas product is sent to the reformer to convert the light hydrocarbons into carbon monoxide and hydrogen. There are two options for gas product reforming, namely steam reforming and partial oxidation. If using steam reforming, it is the same as natural gas steam reforming stated above. If using partial oxidation, oxygen is needed to oxidize the hydrocarbon to hydrogen and carbon monoxide. After reforming, the gas product contains carbon monoxide, hydrogen, carbon dioxide, ammonia, trace amount of unreacted hydrocarbons, water, as well as some embedded solid particles and acid gas. The gas product after reforming is then sent to gas clean-up units to remove the solid particles, ammonia and the hydrocarbons. Similarly, there are two alternatives: cool clean-up and hot clean-up. Specifically, cool clean-up is for high-temperature gasification, whereas hot clean-up is for low-temperature clean-up. Cool clean-up is composed of a filter and two expansions, indicating solid removal first and then expansion to release heat for lowering the temperature. For hot clean-up, the solid in gas product is removed in the scrubber and then compressed to increase the pressure. After gas clean-up, the gas components are hydrogen, carbon monoxide, carbon dioxide, water, ammonia, and hydrocarbons. Such gas mixture is then sent to PSA3 for purification, and the purified product components are hydrogen, carbon monoxide, carbon dioxide, and water. Finally, the PSA product goes to the water gas shift reactor for conversion of carbon monoxide to carbon dioxide, producing hydrogen. The membrane separation is used to purify the product gas and finally supply the high purity hydrogen for hydroprocessing.

Note that the selections of hydroprocessing feedstock options and hydrogen production options are not independent. When hydroprocessing feedstock option (a) is chosen, the hydrogen can be produced from natural gas or biomass other than biocrude, because all biocrude performs as hydroprocessing feed. Specifically, when biomass is chosen for hydrogen production, there are two options for gasification and two options for hydrocarbon reforming. Otherwise, when hydroprocessing feedstock option (b) or (c) is chosen, hydrogen can be only produced from part of biocrude, regardless of natural gas or biomass. Therefore, a total of $1 \times (1 + 2 \times 2) + 1 + 1 = 7$ alternative hydrogen production pathways are available.

Economic and Environmental Impact Analysis

Economic performance of the biorefinery is evaluated by NPV, which is the sum of a series of discounted cash flows, both incoming and outgoing, over the lifetime of the project.[35] The incoming cash flows of the biorefinery include sales of gasoline and diesel products, as well as construction and volumetric incentives from the government.[36] The outgoing cash flows of the biorefinery include total project investment cost (TPIC), operating and maintenance (O & M) cost, as well as federal and state taxes. For incomes, the sales revenue and volumetric incentive are calculated on an annual basis, whereas the construction incentive is a one-time investment. For expenses, the TPIC is a one-time investment at the beginning of the project while the O & M cost and tax are calculated annually. The NPV is calculated as follows: all annual incomes and expenses are discounted according to the present value and then summed up with the one-time incomes and expenses.

As for environmental sustainability of the biorefinery, GWP is used as the indicator to assess the impact of the GHG emissions to the environment. The GHGs considered in this article include carbon dioxide, methane, ethane, propane, and butane. Carbon dioxide is considered the reference for GWP evaluation, thus with the factor of 1. The GWP of other GHGs are converted to the equivalent carbon dioxide by multiplying a factor according to the IPCC 2007 standard.[37] The emissions associated with different components of the biorefinery (e.g., transportation, steam, natural gas, electricity, heat, and direct emissions) are evaluated according to the process-based LCA procedure.[38] By incorporating LCA into a multiobjective superstructure optimization of the hydrocarbon biorefinery, we conduct a "gate-to-gate" LCO, which has been widely used in the sustainable design of biorefinery systems.[21–23,39–42] Though the economic performance of a biorefinery is critical to its viable standing in the marketplace, the environmental sustainability issues cannot be overlooked. LCA[43–46] is the standard procedure to evaluate the environmental performance of a product system.[47,48] The typical process-based LCA follows a four-step procedure.[38] The first step includes setting the boundaries for the LCA analysis, defining the objective, functional unit, and environmental metrics. In the second step, LCI is developed by

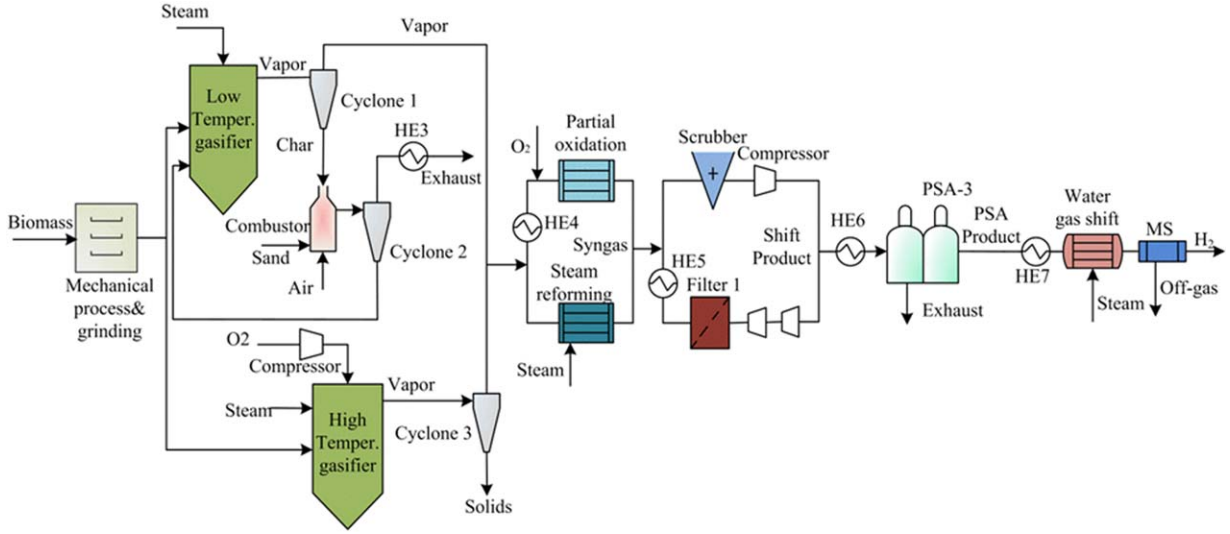

Figure 6. Process flow diagram of hydrogen production from biomass gasification.

[Color figure can be viewed in the online issue, which is available at wileyonlinelibrary.com.]

identification and quantification of the energy and material used in the process. The third step is to evaluate the waste released to the environment associated with the energy and material use. This information is further translated into a set of environmental indicators, which can be used to assess the sustainability of a biorefinery design. The last step is the result summary and report generation. However, traditional LCA cannot automatically generate design alternatives and identify the optimal one. Therefore, to overcome the drawback, LCO framework, which integrates LCA with multiobjective optimization as shown in Figure 7, is used in this work.[43]

Problem Statement

The problem to be addressed in this article is stated in this section. The composition of biomass feedstock, product species coming out of each unit and species distribution of certain units, split fractions of nonreaction units, capacities of each unit, as well as the economic and environmental data are given. Our goal is to propose an optimization model to determine the optimal design and operation of a fast pyrolysis biorefinery while simultaneously maximizing the economic performance and minimizing the environmental impact. Detailed presentation of the assumptions, parameters, objectives, and decision variables considered in the proposed model are given as follows.

Assumptions

1. The ash content is negligible compared to char, thus not included in the model.
2. A linear relationship is assumed between the flow rate of feed streams, and heat and power consumptions of the biorefinery units.[17]
3. The split fractions of species for nonreacting processes and product distributions of the reacting units of the hydrocarbon biorefinery are retrieved from modeling results of similar processes.[12,28–30]
4. For steam reforming, using biocrude or natural gas as feedstock requires the same process.
5. For hydroprocessing, different reactions, feedstocks and catalysts can be performed in the same hydrotreaters and hydrocracker as that in the report by Jones et al.[12]
6. The equipment cost associated with hydrogen production from biomass feedstock is estimated using the base case data in the report by Jones et al.[12]
7. The slight difference in the composition of gasoline and diesel produced by different options is neglected.
8. Considering the scope of this work, average value of the hydrocarbon biofuels selling price, purchase cost of feedstock,

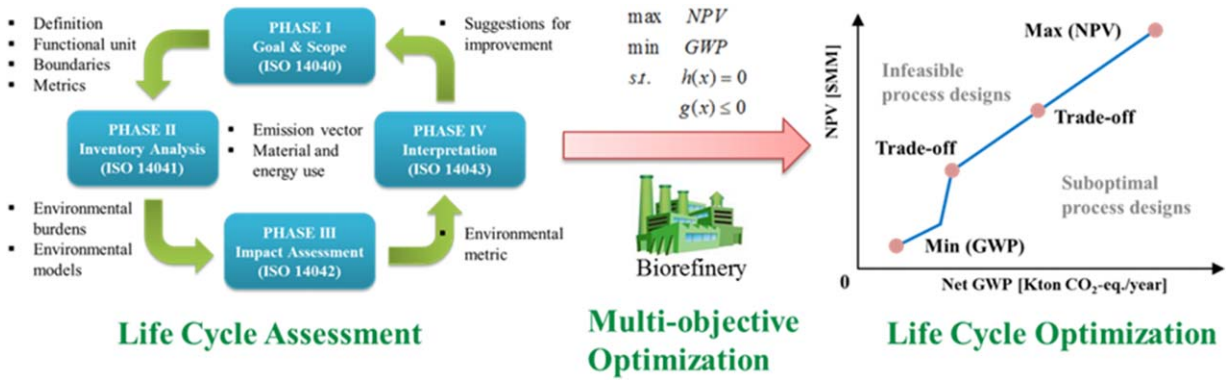

Figure 7. LCA connected with multiobjective optimization.[22]

[Color figure can be viewed in the online issue, which is available at wileyonlinelibrary.com.]

natural gas, heat and electricity are considered. Moreover, the environmental data per functional units retrieved from the environmental databases[49,50] are assumed at their nominal values. However, the proposed model is general enough to account for any variability of these parameters.

Parameters

1. Operating conditions, including temperature, pressure, and properties of feed and product streams for each unit.
2. Product components of each reactor.
3. Split fraction of each separation unit.
4. Electricity consumption per unit flow rate of the compressors and pumps. Heat consumption per unit flow rate of each heat exchanger.
5. The prices of all utilities, including steam, heat, and electricity. Also, prices of natural gas and biomass.
6. Biomass acquisition cost.
7. Capital cost, including equipment purchase, installation, instrumentation and control, piping, electrical system installations, buildings, engineering, construction, legal and contractors fee, project contingency, maintenance cost, working capital, local tax, and insurance factors in terms of percentage of the total equipment purchase cost.
8. The cost of base case equipment purchase, the base case flow rate and the sizing factor of each equipment unit. Besides, chemical engineering plant cost index for each unit to account for the equipment purchase cost inflation relative to the current year.
9. The hydrocarbon biorefinery lifetime. The lower and upper limits of productivity. Income tax and discount rate throughout the project.
10. The selling prices of gasoline and diesel. The incentive value per volumetric biofuels in dollar per gallon. Percentage and maximum allowable construction incentive.
11. Life cycle emissions inventory per functional unit associated with each emissions source category.

Objectives and decision variables

The goal is to determine the optimal design of the sustainable hydrocarbon biorefinery and the corresponding operating conditions that simultaneously maximizes the NPV and minimizes the GWP subject to the constraints for mass balance, energy balance, economic analysis, and environmental evaluation. The major optimization decision variables are listed below.

1. Binary variables for the selection of process design, including process technology pathways, equipment units and their interconnections.
2. Production capacity of the hydrocarbon biorefinery and the size of each processing unit involved in the hydrocarbon biorefinery.
3. The molar or mass flow rates of species and streams at all the units in the process, such as crude bio-oil intermediate, off-gas for hydrogen production, and hydrogen products.
4. Hydrocarbon biofuels yield, feedstock, steam, electricity, and natural gas consumption rates.
5. Cost of each unit, annualized investment cost and annual operating cost, total cost.
6. Total emission, including natural gas, electricity, biomass transportation, steam, heat, and direct emission.

Model Formulation and Solution Method

The mathematical model formulated in this work is a bi-criteria MINLP problem, which determines the optimal design and operation of the hydrocarbon biorefinery under the economic and environmental objectives. Considering the length of the article, detailed mathematical model and notations are presented in Supporting Information.

In the mathematical model formulation, four major types of constraints are considered, namely, mass balance constraints (1)–(135), energy balance constraints (136)–(140), economic analysis constraints (141)–(159), and environmental impact analysis constraints (160)–(163). Mass balance constraints perform species balance for each unit and atomic balance for units involving chemical reactions. Split fractions of columns and reaction parameters are retrieved from open literatures. The only nonlinear relationship in mass balance constraints is the water gas shift reaction Eqs. 74, 78, 125, 130, and 131. Energy balance constraints include heat consumption, heat generation, and power generation. Heat change of a unit is calculated by the total enthalpy differences between inlet and outlet streams. Power generation is estimated by linearly scaling an existing device. As for economic analysis, its goal is to evaluate the NPV from total investment cost, incentives, and revenue on the basis of mass balance and energy balance variables. The capital cost of each equipment is estimated using nonlinear sizing equations. Finally, environmental impact analysis quantifies GWP of each interested category as the product of life cycle inventories and corresponding damage factors and the total GWP is the sum of all GWPs. The NPV is more computational demanding due to its nonlinear features, whereas GWP is formulated as a linear function and consumes less computation resource. Ultimately, both objective functions are embedded in the MINLP multiobjective framework and solved together using ε-constraint method.

Problem (P) shows generic formulation of the given problem. Two objectives are maximizing the NPV and minimizing the GWP, respectively. The constraints involve both equalities and inequalities. The equalities often represent the mass and energy balance constraints, as well as equations related to cost evaluation and LCA. The inequalities mostly correspond to the design specifications (e.g., capacity limits and process variable bounds). The continuous variables represent the flow rates, capacities, and so forth. The binary 0–1 variables indicate the selection of technologies, catalysts, feedstock options, and so forth.

$$
(\mathbf{P}) \quad \begin{aligned} &\max && \text{NPV} \\ &\min && \text{GWP} \\ &\text{s.t.} && h(x)=0 \\ & && g(x) \le 0 \\ & && x \in \Re \cup \{0,1\} \end{aligned}
$$

Since multiple objectives are involved in the proposed mathematical model, conventional single-objective optimization methods cannot be applied directly. Among the various multiobjective optimization methods, ε-constraint method is proved to be efficient and straightforward to formulate.[51] Therefore, we use the ε-constraint method to solve the proposed bi-criteria MINLP problem. According to the ε-constraint method, the Pareto-optimal solutions of problem (P) can be obtained by solving a series of subproblems (PR) with different values of the ε-parameter.

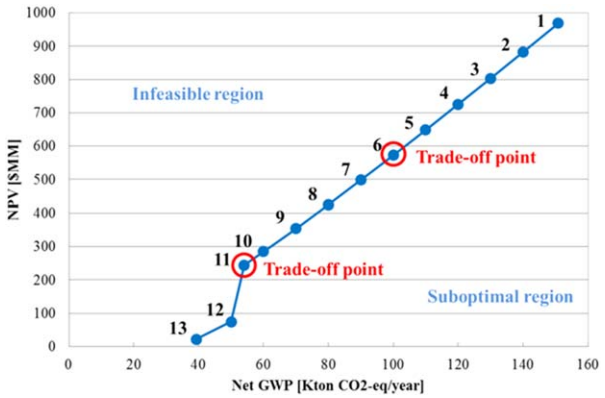

Figure 8. Pareto-optimal solutions of biorefinery design through pyrolysis and hydroprocessing.

[Color figure can be viewed in the online issue, which is available at wileyonlinelibrary.com.]

$$
(\mathbf{PR}) \quad \begin{aligned} &\max && \text{NPV} \\ &\text{s.t.} && \text{GWP} \le \varepsilon \\ & && h(x)=0 \\ & && g(x) \le 0 \\ & && x \in \Re \cup \{0,1\} \end{aligned}
$$

Results and Discussion

The MINLP model is coded in GAMS 24.0.2.[52] All the computational studies were performed on a DELL OPTIPLEX 790 desktop with Intel(R) Core(TM) i5–2400 CPU @ 3.10GHz and 4 GB RAM, using windows 7 64 bit operating system. The optimization problem involves 12 binary variables, 1597 continuous variables, and 1956 equations. The MINLP problem is solved using BARON 10.2.0[53] to achieve the global optimality with 0% relative gap. All 13 Pareto-optimal points are obtained in 10,800 CPU seconds.

Pareto-optimal designs

Figure 8 gives the Pareto curve, in which 13 design points are included. In this figure, vertical coordinate is the NPV in unit of $MM, whereas horizontal coordinate is the GWP in unit of kton CO_2-eq/year. This curve shows the trade-off between economic performance and environmental evaluation. The points on this curve are all Pareto-optimal, where the NPV is maximized with respect to the specified GWP limit. Solutions in the region above the curve are infeasible, whereas solutions in the region below the curve are feasible but suboptimal.

Each point on the Pareto curve represents an optimal design and operation of the biorefinery. Point 1 on the top right has the maximum NPV among all the feasible solutions, where all the biocrude is fed to hydroprocessing and hydrogen is produced by natural gas steam reforming. On point 1, the NPV is $968.4 MM and the corresponding GWP is 150.8 kton CO_2-eq/year. The unit production cost of biofuels is $3.13/GGE and the emission is 1.95 kg CO_2-eq/GGE. In contrast, point 13 on the bottom left has the minimum GWP, where part of the biocrude is utilized for hydroprocessing with NiMo catalyst and the remaining part is sent to steam reforming for hydrogen production. On point 13, the NPV is $22.1 MM and the corresponding GWP is 39.2 kton CO_2-eq/year. The unit production cost of biofuels is $5.76/GGE and the emission is 2.05 kg CO_2-eq/GGE. Point 10 is a turning point on the Pareto curve, indicating change in the process design. The Pareto curve between point 1 and point 11 is a straight line which indicates these optimal solutions have the same the binary decisions and the only major difference among them is the plant capacity. In other words, they have the same process design where hydroprocessing feedstock option (a) is chosen and hydrogen is produced from natural gas steam reforming. However, the solutions between point 11 and 13 have the process design where hydroprocessing feedstock option (c) is chosen and hydrogen is produced from the biocrude. Note that, none of the Pareto-optimal solutions select the hydrogen production from biomass. This is because producing hydrogen from biomass requires a higher capital cost compared to that from natural gas. Conversely, producing hydrogen from biomass leads to a higher GHG emissions compared to that from biocrude because of the higher utility consumption, including power and steam.

The total annualized cost distribution for all the 13 Pareto-optimal solutions are presented in Figure 9. The vertical coordinate is the total cost in the unit of $MM and the horizontal coordinate corresponds to the 13 Pareto points. The dark part (bottom) of the columns stands for the annualized investment cost and the light part (top) of the columns represents the annual operating cost.

For the first 10 points, the total annual cost decreases from $241.2 MM to $121 MM. For points 11–13, the design is changed and the total annualized cost drops from $140 MM to $110 MM. A linear decrease in the total cost can be observed from points 1–10. This is because the same design is selected. The difference is only in the capacity of the biofuel production process.

Process yield and consumption

Here we select two representative Pareto-optimal solutions for further discussion, namely point 6 and point 11, which are denoted as trade-off points in Figure 8. At point 6, the NPV is 59.2% of the maximum value, whereas GWP is

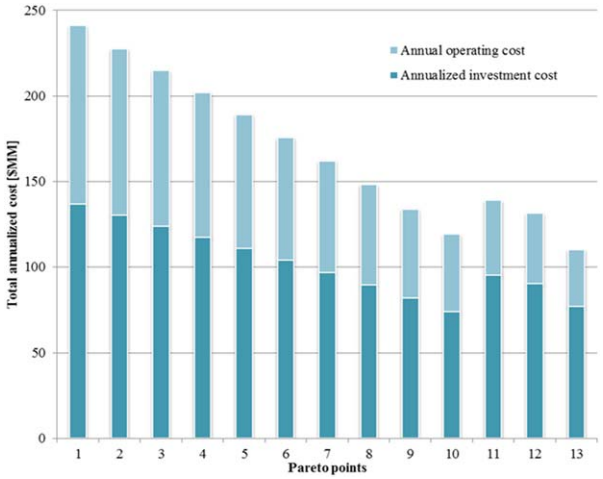

Figure 9. Total annual cost distribution for each Pareto point.

[Color figure can be viewed in the online issue, which is available at wileyonlinelibrary.com.]

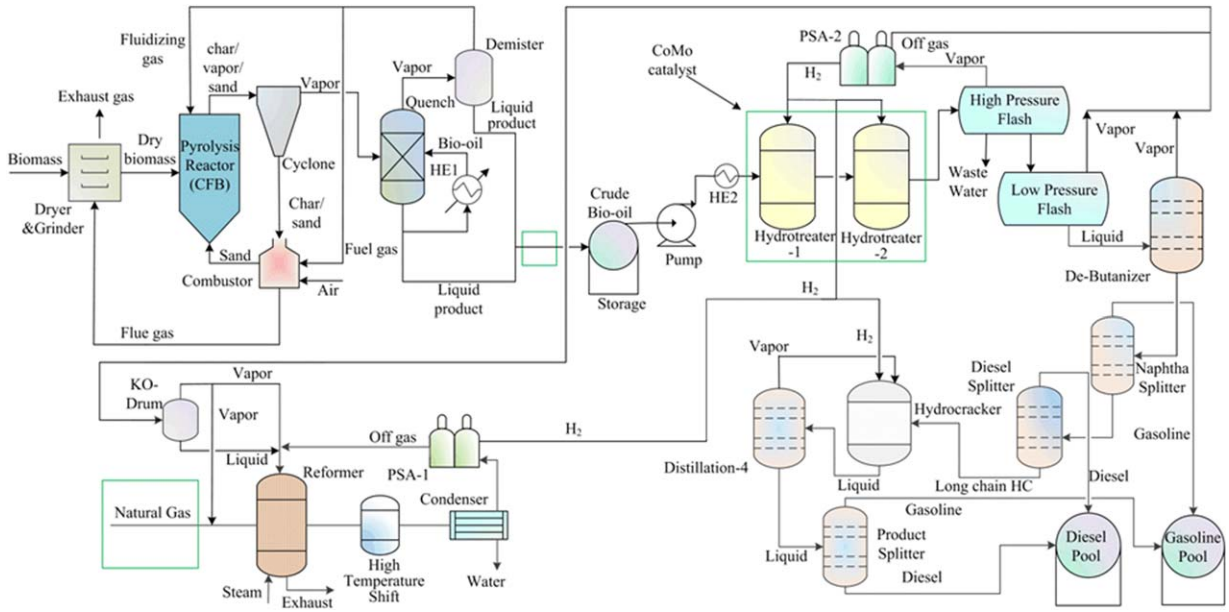

Figure 10. Process design of the biorefinery with all biocrude utilization for hydroprocessing and hydrogen production from natural gas (point 6).

[Color figure can be viewed in the online issue, which is available at wileyonlinelibrary.com.]

reduced by 33.3% compared to that of the maximum NPV design. The process flow diagram of this optimal biorefinery design is shown in Figure 10. If a more stringent GHG restriction is imposed, point 11 might be a proper solution that trades off the economic and environmental performances. The NPV of point 11 increases significantly at merely a slight compromise in GWP, compared to that of point 13. The process diagram of point 11 is shown in Figure 11. The NPV, GWP, unit production cost, unit GHG emission, biomass feedstock processing capacity, unit hydrogen consumption, unit steam consumption, power consumption, fuel productivities of gasoline and diesel for both designs in Figures 10 and 11 are summarized in Table 1.

The differences between Figures 10 and 11 are in the hydroprocessing feedstock and hydrogen production options, as shown by the green rectangles. Note that the separator placed in the middle of Figure 11 is used to separate the water soluble oil from biocrude. All the biocrude is utilized for hydroprocessing with CoMo catalyst in Figure 10, whereas only part of the biocrude is utilized in Figure 11 corresponding to the UOP technology with NiMo catalyst. Consequently, hydrogen is produced from natural gas in

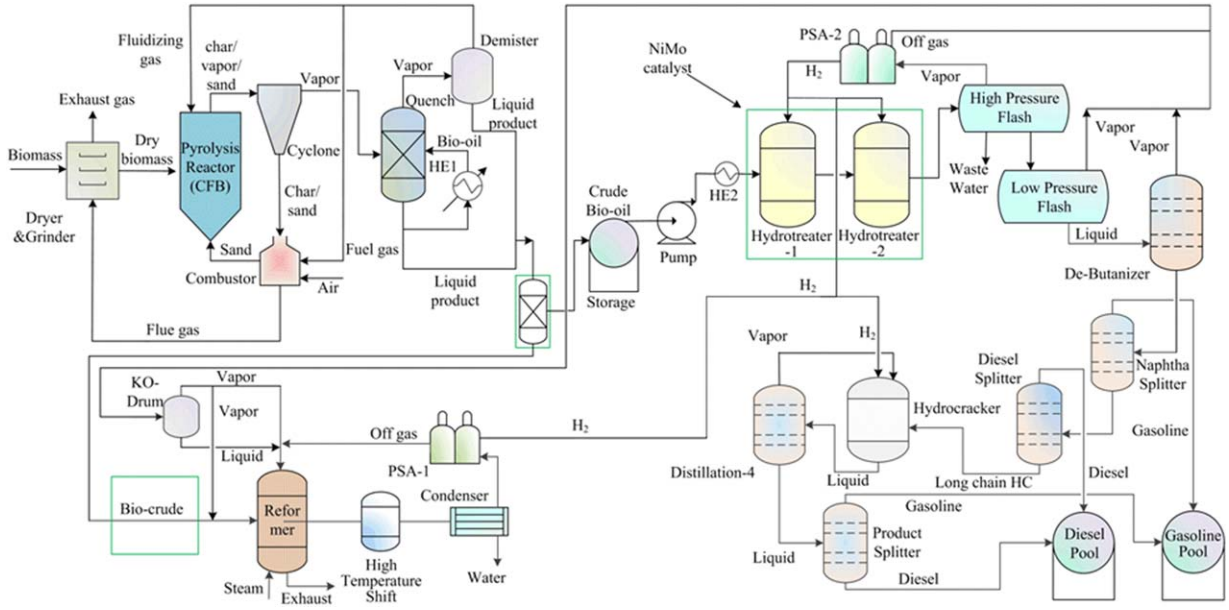

Figure 11. Process design of the biorefinery with partial biocrude utilization for hydroprocessing and hydrogen production from partial biocrude (point 11).

[Color figure can be viewed in the online issue, which is available at wileyonlinelibrary.com.]

Table 1. Results Comparison Between the Two Selected Optimal Designs

Process Designs	Point 6 Hydroprocessing: Feed Option 1, Hydrogen Production: Natural Gas	Point 11 Hydroprocessing: Feed Option 3, Hydrogen Production: Biocrude
NPV ($MM)	573	93.6
GWP (kton CO_2-eq/year)	100	53
Unit production cost ($/GGE)	3.43	5.26
Unit GHG emission ($kgCO_2$-eq/GGE) eq/GGE)	1.95	2.04
Dried feedstock (kg/day)	1,330,000	992,000
Unit H_2 consumption (kg/GGE)	0.33	0.31
Steam consumed (kg/GGE)	3.81	7.22
Power consumed (MW)	9.04	5.94
Natural gas (kg/day)	128,500	0
Gasoline produced (M gallon/year)	22.1	17.6
Diesel produced (M gallon/year)	25.6	7.7

Figure 10, whereas that in Figure 11 is from part of the biocrude. From the comparison in Table 1, although the NPV, unit production cost, biofuels productivity, steam and power costs in the design of Figure 10 are superior to that in Figure 11, the unit GHG emission is almost the same between the two designs, and furthermore, the natural gas and unit hydrogen comsumptions in the design of Figure 11 are both better than that in Figure 10.

From the cost perspective, Figure 12 presents the break down of annual operating cost for the two cases of maximum NPV (point 1) and minimum GWP (point 13),

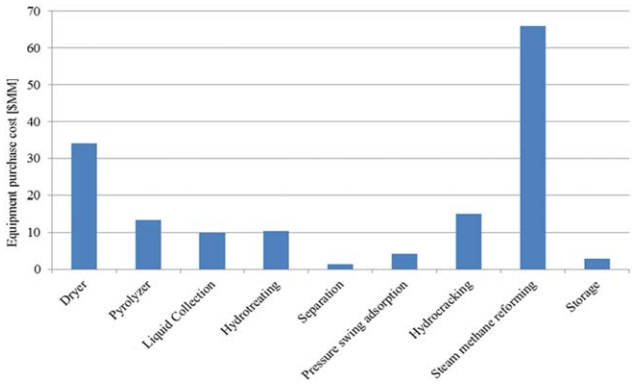

Figure 13. Equipment purchase cost distribution for the case of maximum NPV (point 1).

[Color figure can be viewed in the online issue, which is available at wileyonlinelibrary.com.]

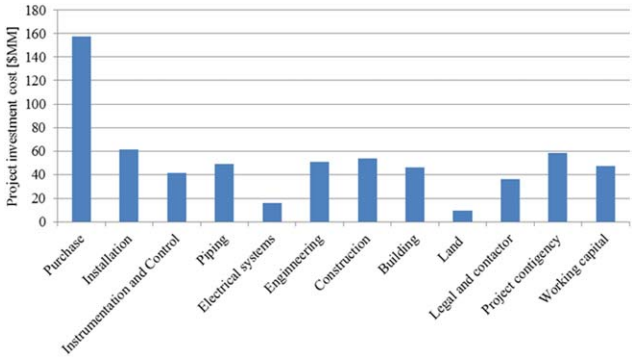

Figure 14. TPIC distribution for the case of maximum NPV (point 1).

[Color figure can be viewed in the online issue, which is available at wileyonlinelibrary.com.]

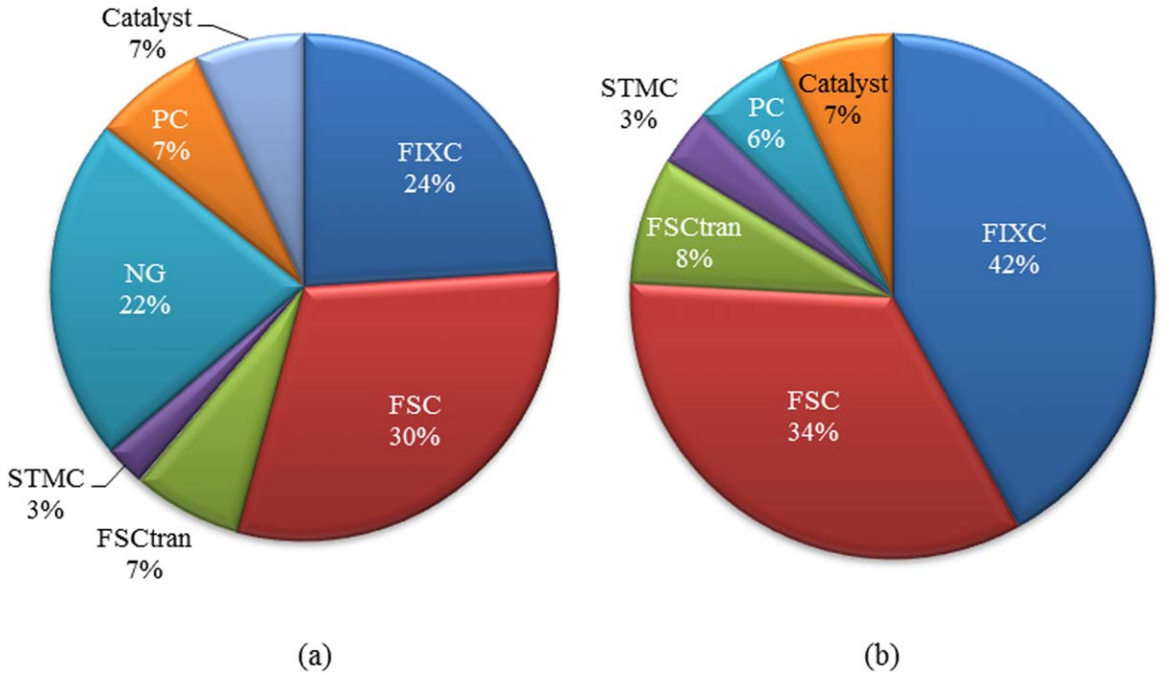

Figure 12. Annual operating cost distribution for (a) maximum NPV and (b) minimum GWP.

Abbreviations: FIXC (fixed O & M cost), FSC (feedstock cost), FSCtran (feedstock transportation cost), STMC (steam cost), NG (natural gas cost), PC (power cost), and Catalyst (catalyst cost). [Color figure can be viewed in the online issue, which is available at wileyonlinelibrary.com.]

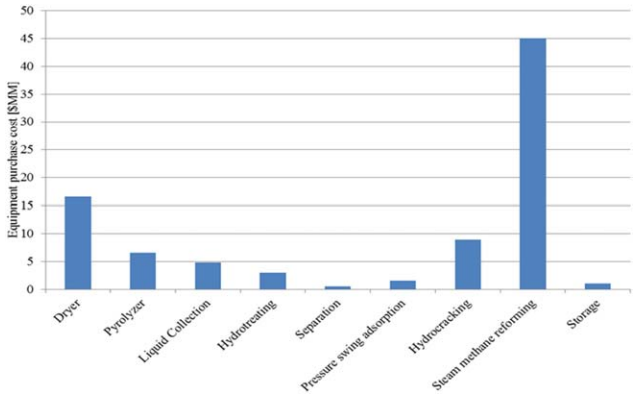

Figure 15. Equipment purchase cost distribution for the case of minimum GWP (point 13).

[Color figure can be viewed in the online issue, which is available at wileyonlinelibrary.com.]

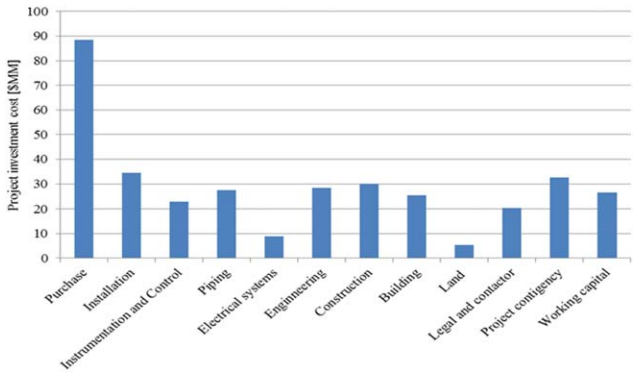

Figure 16. TPIC distribution for the case of minimum GWP (point 13).

[Color figure can be viewed in the online issue, which is available at wileyonlinelibrary.com.]

respectively. As can be seen from Figure 12a, feedstock purchase cost constitutes the largest part (30%) in the cost profile of point 1. The fixed O & M cost and natural gas purchase cost also account for over 20% of the total cost. These three items totally make up 76% of the annual operating cost. In contrast, in the cost profile of point 13 shown by Figure 12b, the fixed O and M cost takes up 42% and feedstock purchase cost takes up 34%. These two items together account for 76% of the total cost. The significant difference between the cost profile of point 1 and 13 is due to the fundamental change in production pathways.

Figures 13 and 14 show the distribution of equipment purchase cost and project investment cost in the case of maximum NPV (point 1). The purchase cost is dominanted by the steam reformer used in the hydrogen production section, which is \$66 MM. The dryer and pyrolyzer used in the pyrolysis section together cost about \$50 MM. The costs of stream reformer, dryer, and pyrolyzer make up 70% of the total equipment purchase cost. The TPIC is \$625.4 MM, in which the equipment purchase cost (\$158 MM) is the main contributor. The other related costs (e.g., installation, instrumentation and control, piping) are proportional to the purchase cost.

Figures 15 and 16 provide the distribution of equipment purchase cost and project investment cost of the case of minimum GWP (point 13), respectively. Similar to the case of maximum NPV, steam reforming and pyrolysis are the two cost-dominant procresses, which costs \$45 MM and \$22 MM, respectively. These two costs make up more than 80% of the total equipment purchase cost. The TPIC is \$351 MM. As can be seen from Figure 16, equipment purchase cost (\$88.2 MM) is dominant among all the investment cost categories.

As for the environmental impact, Figure 17 presents the GHG emission distribution associated with the various materials and activities in the biorefinery, namely biomass transportation, steam, natural gas, electricity, heat, and

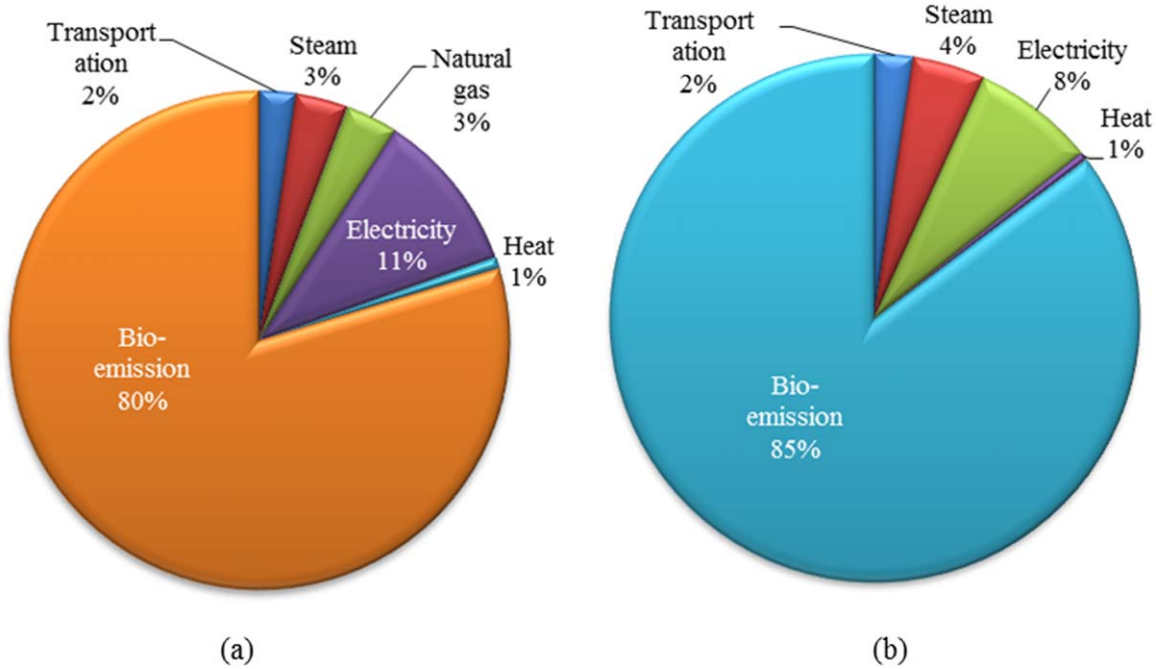

Figure 17. Emission distribution for (a) maximum NPV and (b) minimum GWP.

[Color figure can be viewed in the online issue, which is available at wileyonlinelibrary.com.]

bioemission. Bioemission indicates the biomass-derived direct GHG emissions. As shown in Figure 17a, 80% of the GHG emissions is from bioemission in point 1, mainly including the combustor exhaust gas, steam reformer furnace exhaust, PSA2 exhaust gas, and low pressure flash vents. Note that as natural gas is not used in the minimum GWP design (point 13), there is no emission category associated with natural gas in Figure 17b.

Figures 18 and 19 summarize, respectively, the total annualized cost and GHG emissions at both maximum (2000 dry ton/day) and minimum (720 dry ton/day) capacities from different hydrogen production pathways (namely, natural gas, biomass, and biocrude). As can be seen from Figure 18, if the biorefinery is operating at the maximum biomass processing capacity, the option of hydrogen production from biomass has the highest total annualized cost ($260 MM) among the three pathways. The other two cases are $258 MM and $256 MM, respectively. If the biorefinery is operating at the minimum production capacity, the results are similar. Hydrogen production from biomass is still the highest in total annualized cost, which is about $120 MM. The other two cases are less than $110 MM. As can be observed from Figure 19, at the maximum capacity, the GHG emissions for producing hydrogen from natural gas and biomass are almost the same, at about 150 kton CO_2-eq/year. However, the GHG emissions for producing hydrogen from biocrude is 110 kton CO_2-eq/year, which is much lower than that of the other two cases. Similar results can also be observed in the case of minimum production capacity.

From the comparison of Figures 18 and 19, we know that hydrogen production from biomass is limited by its high investment cost. The bottleneck is at the low conversion (less than 60%) of water gas shift reaction converting carbon monoxide to carbon dioxide. If the conversion can be increased, then for the same amount of hydrogen produced, the plant size and the investment cost will be lowered. For hydrogen production from biocrude, as the reaction can perform in the same infrastructure as that of natural gas, its production cost would be similar but the GHG emissions can be significantly reduced compared to the option of hydrogen production from natural gas. Therefore, producing hydrogen from biocrude might be a promising alternative for the biorefinery design in the future.

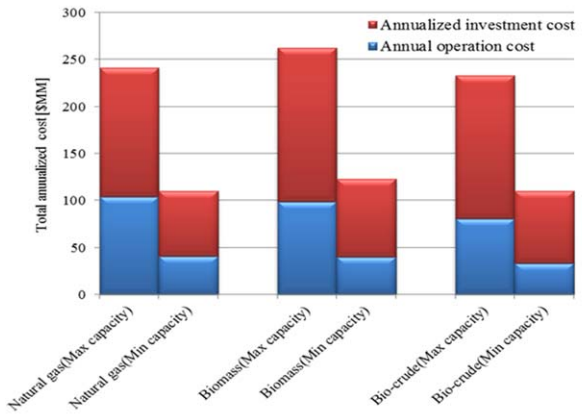

Figure 18. Comparison of the total annualized cost among three hydrogen production options at minimum and maximum capacities.

[Color figure can be viewed in the online issue, which is available at wileyonlinelibrary.com.]

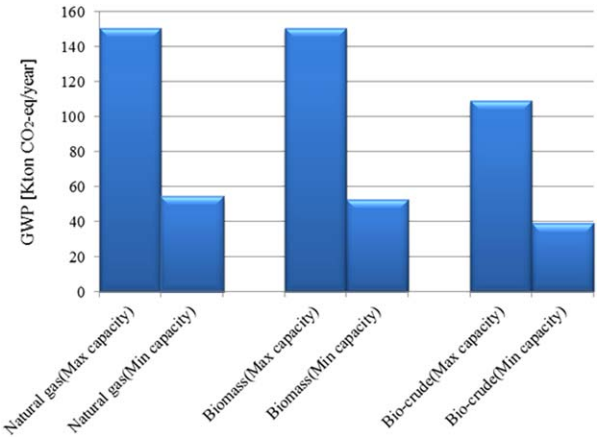

Figure 19. Comparison of GHG emissions among three hydrogen production options at minimum and maximum capacities.

[Color figure can be viewed in the online issue, which is available at wileyonlinelibrary.com.]

Conclusions

We developed a superstructure for the sustainable design and operation of hydrocarbon biorefinery consisting of fast pyrolysis, biocrude collection, hydroprocessing, and hydrogen production sections. A bi-criteria MINLP model was proposed for the optimization of the superstructure. A series of Pareto-optimal solutions were obtained, resulting in a Pareto curve that reveals the tradeoffs between economic and environmental performance in the design and operation of the biorefinery. Two optimal production designs are identified from the results. One is with all biocrude utilized for hydroprocessing using CoMo catalyst and hydrogen production from natural gas steam reforming. The other is with part of the biocrude utilized for hydroprocessing using NiMo catalyst and hydrogen production by steam reforming the other part of the biocrude. The total annualized cost, consisting of total annual operating cost and total annualized investment cost, is $241.2 MM in the maximum NPV design and $110 MM in the minimum GWP design, respectively. In total annual operating cost, fixed O & M and feedstock cost are the two major contributors. In the equipment purchase cost, which is the dominant part of the investment cost, dryer, pyrolyzer, and steam reformer make up more than 70% of the total purchase cost. The unit production cost ranges from $3.13/GGE in the maximum NPV design to $5.76/GGE in the minimum GWP design. From the environmental impact perspective, the total emission is 150.8 kton CO_2-eq/year in the maximum NPV design and 39.2 kton CO_2-eq/year in the minimum GWP design. In both cases, the direct emissions category related to the various biofuel production processes is the major contributor, making up more than 80% of the total GHG emissions. As a considerable amount of hydrogen is required for hydroprocessing, the hydrogen production option is critical to the design of a biorefinery. Three hydrogen production options are considered in this work. Results showed that producing hydrogen from biomass causes a significantly higher cost than that from natural gas or biocrude. The biorefinery design of hydroprocessing part of the

biocrude and hydrogen production from the remaining part of the biocrude indicates less unit hydrogen consumption than that of natural gas and biomass designs. In addition, hydrogen production from biocrude results in lower GHG emissions than that from natural gas and biomass. In summary, a complete modeling framework was provided in this work for the design and operation of a biorefinery that is both economically viable and environmentally sustainable.

Acknowledgment

The financial support from the Initiative for Sustainability and Energy at Northwestern (ISEN) is gratefully acknowledged.

Literature Cited

1. Sadhukhan J, Ng KS. Economic and European union environmental sustainability criteria assesment of bio-oil-based biofuel systems: refinery integration cases. *Ind Eng Chem Res*. 2011;50:6794–6808.
2. Sissine F. *Energy Independence and Security Act of 2007: A Summary of Major Provisions*, Washington, DC: Congressional Research Service, The Library of Congress, 2007.
3. DOE/EERE. *U.S. Billion-Ton Update: Biomass Supply for a Bioenergy and Bioproducts Industry*. ORNL/TM-2011/224. Oak Ridge, TN: Oak Ridge National Laboratory, 2011:227.
4. MASBI. Fueling a sustainable future for aviation. Midwest Aviation Sustainable Biofuels Initiative, 2013. Available at: www.masbi.org, accessed on January 9, 2013.
5. DOE/EERE. *Thermochemical Conversion: Using Heat and Chemistry to Make Fuels and Bioproducts*. U.S. Department of Energy, Office of Energy Efficiency & Renewable Energy, Washington, DC, 2011.
6. Yue D, You F, Snyder SW. Biomass-to-bioenergy and biofuel supply chain optimization: overview, key issues and challenges. *Comput Chem Eng*. In press. DOI: 10.1016/j.compchemeng.2013.1011.1016.
7. Cano-Ruiz J, McRae G. Environmentally conscious chemical process design. *Annu Rev Energy Environ*. 1998;23:499–536.
8. Bridgwater AV. Review of fast pyrolysis of biomass and product upgrading. *Biomass Bioenergy*. 2012;38:68–94.
9. Tanksale A, Beltramini JN, Lu GM. A review of catalytic hydrogen production processes from biomass. *Renewable Sustain Energy Rev*. 2010;14:166–182.
10. Swanson RM, Satrio JA, Brown RC, Platon A, Hsu DD. *Techno-Economic Analysis of Biofuels Production Based on Gasification*. Golden, CO: National Renewable Energy Laboratory, Technical Report, 2010.
11. Swanson RM, Platon A, Satrio JA, Brown RC. Techno-economic analysis of biomass-to-liquids production based on gasification. *Fuel*. 2010;89:S11–S19.
12. Jones SB, Valkenburg C, Walton CW, Elliott DC, Holladay JE, Stevens DJ, Kinchin C, Czernik S. *Production of Gasoline and Diesel from Biomass via Fast Pyrolysis, Hydrotreating and Hydrocracking: A Design Case*. Richland, WA: Pacific Northwest National Laboratory, 2009.
13. Wright MM, Daugaard DE, Satrio JA, Brown RC. Techno-economic analysis of biomass fast pyrolysis to transportation fuels. *Fuel*. 2010; 89:S2–S10.
14. Sammons NE Jr, Yuan W, Eden MR, Aksoy B, Cullinan HT. A systematic framework for biorefinery production optimization. *Comput Aided Chem Eng*. 2008;25:1077–1082.
15. Liu P, Pistikopoulos EN, Li Z. A multi-objective optimization approach to polygeneration energy systems design. *AIChE J*. 2010; 56:1218–1234.
16. Chen Y, Adams TA, Barton PI. Optimal design and operation of flexible energy polygeneration systems. *Ind Eng Chem Res*. 2011;50: 4553–4566.
17. Chen Y, Adams TA, Barton PI. Optimal design and operation of static energy polygeneration systems. *Ind Eng Chem Res*. 2010;50: 5099–5113.
18. Baliban RC, Elia JA, Floudas CA. Optimization framework for the simultaneous process synthesis, heat and power integration of a thermochemical hybrid biomass, coal, and natural gas facility. *Comput Chem Eng* 2011;35:1647–1690.
19. Martín M, Grossmann IE. Energy optimization of bioethanol production via gasification of switchgrass. *AIChE J*. 2011;57:3408–3428.
20. Martín M, Grossmann IE. Process optimization of FT-diesel production from lignocellulosic switchgrass. *Ind Eng Chem Res*. 2011;50: 13485–13499.
21. Wang B, Gebreslassie BH, You F. Sustainable design and synthesis of hydrocarbon biorefinery via gasification pathway: integrated life cycle assessment and technoeconomic analysis with multiobjective superstructure optimization. *Comput Chem Eng* 2013;52:55–76.
22. Gebreslassie BH, Slivinsky M, Wang B, You F. Life cycle optimization for sustainable design and operations of hydrocarbon biorefinery via fast pyrolysis, hydrotreating and hydrocracking. *Comput Chem Eng*. 2013;50:71–91.
23. Gebreslassie BH, Waymire R, You F. Sustainable design and synthesis of algae-based biorefinery for simultaneous hydrocarbon biofuel production and carbon sequestration. *AIChE J*. 2013;59:1599–1621.
24. Daoutidis P, Marvin WA, Rangarajan S, Torres AI. Engineering biomass conversion processes: a systems perspective. *AIChE J*. 2013; 59:3–18.
25. El-Halwagi AM, Rosas C, Ponce-Ortega JM, Jimenez-Gutierrez A, Mannan MS, El-Halwagi MM. Multiobjective optimization of biorefineries with economic and safety objectives. *AIChE J*. 2013;59: 2427–2434.
26. Pham V, El-Halwagi M. Process synthesis and optimization of biorefinery configurations. *AIChE J*. 2012;58:1212–1221.
27. Ng RTL, Hassim MH, Ng DKS. Process synthesis and optimization of a sustainable integrated biorefinery via fuzzy optimization. *AIChE J*. 2013;59:4212–4227.
28. Marker T. *Opportunities for Biorenewables in Oil Refineries*. Des Plaines, IL: UOP LLC, 2005.
29. Elliott DC, Hu J, Hart TR, Neuenschwander GG. Palladium catalyzed hydrogenation of bio-oils and organic compounds, Google Patents (US 7425657 B1), 2011.
30. Marker TL, Petri JA. Gasoline and diesel production from pyrolytic lignin produced from pyrolysis of cellulosic waste, Google Patents (WO 2008027699 A2), 2009.
31. Tong K, Gong J, Yue D, You F. Stochastic programming approach to optimal design and operations of integrated hydrocarbon biofuel and petroleum supply chains. *ACS Sustain Chem Eng*. 2014;2(1): 49–61.
32. Wang D, Czernik S, Montane D, Mann M, Chornet E. Biomass to hydrogen via fast pyrolysis and catalytic steam reforming of the pyrolysis oil or its fractions. *Ind Eng Chem Res*. 1997;36:1507–1518.
33. Martín M, Grossmann IE. Energy optimization of hydrogen production from lignocellulosic biomass. *Comput Chem Eng*. 2011;35: 1798–1806.
34. Lau FS, Bowen DA, Dihu R, Doong S, Hughes EE, Remick R, Slimane R, Turn SQ, Zabransky R. Techno-Economic Analysis of Hydrogen Production by Gasification of Biomass. Department of Energy and National Renewable Energy Laboratory, DE-FC36-01GO11089, Washington, DC, 20585, 2003.
35. Wikipedia. Net present value. *Wikipedia The Free Encyclopedia*. Available at: http://en.wikipedia.org/wiki/Net_present_value, accessed on January 9, 2013.
36. DOE/EERE. *Federal and State Laws and Incentives*. U.S. Department of Energy, Office of Energy Efficiency & Renewable Energy. Washington, DC. Available at: http://www.afdc.energy.gov/laws/, accessed on July 19, 2013.
37. Solomon S. *Climate Change 2007: Contribution of Working Group I to the Fourth Assessment Report of the Intergovernmental Panel on Climate Change*. Cambridge, UK: Cambridge University Press, 2007.
38. Goedkoop M, Spriensma R. *The Eco-Indicator99: A Damage Oriented Method for Life Cycle Impact Assessment: Methodology Report*, Amersfoort, Netherlands: Pré Consultants BV, 2001.
39. You F, Tao L, Graziano DJ, Snyder SW. Optimal design of sustainable cellulosic biofuel supply chains: multiobjective optimization coupled with life cycle assessment and input–output analysis. *AIChE J*. 2012;58:1157–1180.
40. You F, Wang B. Life cycle optimization of biomass-to-liquid supply chains with distributed–centralized processing networks. *Ind Eng Chem Res*. 2011;50:10102–10127.
41. Yue D, Kim MA, You F. Design of sustainable product systems and supply chains with life cycle optimization based on functional unit: general modeling framework, mixed-integer nonlinear programming algorithms and case study on hydrocarbon biofuels. *ACS Sustain Chem Eng*. 2013;1:1003–1014.

42. Gebreslassie BH, Yao Y, You FQ. Design under uncertainty of hydrocarbon biorefinery supply chains: multiobjective stochastic programming models, decomposition algorithm, and a comparison between CVaR and downside risk. *AIChE J*. 2012;58:2155–2179.
43. Azapagic A. Life cycle assessment and its application to process selection, design and optimisation. *Chem Eng J*. 1999;73:1–21.
44. Azapagic A, Clift R. The application of life cycle assessment to process optimisation. *Comput Chem Eng*. 1999;23:1509–1526.
45. Yue D, You F. Sustainable scheduling of batch processes under economic and environmental criteria with MINLP models and algorithms. *Comput Chem Eng*. 2013;54:44–59.
46. Azapagic A, Clift R. Life cycle assessment and multiobjective optimisation. *J Cleaner Prod*. 1999;7:135–143.
47. Cano-Ruiz JA, McRae GJ. Environmentally conscious chemical process design. *Annu Rev Energy Environ*. 1998;23:499–536.
48. IRAM-ISO-14040. *Environmental Management—Life Cycle Assessment—Principles and Frame Work*, International Standard: ISO, Scotts Valley, CA: Stadler-Burgess, 2006.
49. Center E. A Competence Centre of ETH. PSI, Empa and ART. Ecoinvent Data Swiss Centre for Life Cycle Inventories, ETH Zurich, v2, Dübendorf, Switzerland: Swiss Centre for Life Cycle Inventories, 2009:12009.
50. Wang M. *The Greenhouse Gases, Regulated Emissions, and Energy Use in Transportation (GREET) Model: Version 1.5*. Center for Transportation Research, Lemont, IL: Argonne National Laboratory, 2008.
51. Ehrgott M. *Multicriteria Optimization*. Berlin, Heidelberg: Springer, 2005.
52. Rosenthal RE. *GAMS—A User's Guide*. Washington, DC: GAMS Development Corp., 2011.
53. Tawarmalani M, Sahinidis NV. A polyhedral branch-and-cut approach to global optimization. *Math Program*. 2005;103:225–249.

Manuscript received Sept. 3, 2013, and revision received Dec. 17, 2013.